Simultaneous in-Situ Monitoring of Parallel Polymerization Reactions Using Light Scattering; A New Tool for High-Throughput Screening

4 AUTHORS, INCLUDING:

Michael F. Drenski
Tulane University
19 PUBLICATIONS **133** CITATIONS

SEE PROFILE

Emmanuel Mignard
French National Centre for Scientific Research
21 PUBLICATIONS **272** CITATIONS

SEE PROFILE

Alina M Alb
46 PUBLICATIONS **595** CITATIONS

SEE PROFILE

Simultaneous in-Situ Monitoring of Parallel Polymerization Reactions Using Light Scattering; A New Tool for High-Throughput Screening

Michael F. Drenski, Emmanuel Mignard,[†] Alina M. Alb, and Wayne F. Reed*

Physics Department, Tulane University, New Orleans, Louisiana 70118

A recently introduced technique, simultaneous multiple sample light scattering (SMSLS), was used to monitor parallel polymerization reactions in situ. SMSLS is designed for real-time, high-throughput screening and provides a time-dependent light scattering signature for each reaction, which contains both qualitative and semiquantitative information. Qualitatively, the signature immediately indicates whether the reaction occurs or not, whether there is an initial lag period, and how long the reaction takes until it stops. The signature also provides estimates of the reaction rate and weight average molecular mass M_w, and its shape can help identify mechanistic aspects, for example, controlled versus free radical polymerization, presence of impurities, etc. The method is inherently adapted to small sample volumes and requires no special sample preparation or postpolymerization characterization. The demonstration here involved the free radical polymerization of acrylamide under varying conditions and should be readily applicable to a wide variety of other reactions. Results were cross-checked with multi-detector gel permeation chromatography.

Introduction

New materials and methods for synthesizing and characterizing novel polymers are appearing at a rapid rate.[1−4] Often, the bottleneck in the evaluation of new polymers is the ability to rapidly screen the results of many reactions to see if certain minimum criteria are being met; for example, does the reaction occur at all, and, if so, what is the rate and the time scale for completion, what is the approximate weight average molar mass of the polymer M_w, and so on. Reactions that meet the minimum criteria may subsequently be studied in more detail. In the screening process, it is hence not necessary to know rates or M_w to high precision. A combination of qualitative indicators, together with some estimates of magnitude, will often suffice for screening purposes.

Simultaneous multiple sample light scattering (SMSLS) was recently introduced[5−7] and permits independent samples to be monitored at the same time. It was demonstrated that SMSLS could make absolute M_w determinations of polymers in dilute solution to a precision of better than 2% and also be used to follow aggregation and degradation kinetics. In this work, SMSLS is used to approach the high-throughput screening problem in polymer synthesis. As mentioned, the goal is not to obtain absolute, precise kinetics of each reaction monitored simultaneously, but rather to obtain the type of qualitative and semiquantitative information necessary for rapid screening.

To screen different polymerization reactions in situ, SMSLS is adapted to small reactor volumes. This could be important in areas such as cosmetics or biochemistry where expensive chemicals may be used. Because SMSLS is noninvasive (light merely scatters from the sample without affecting it), each polymerization product can be fully recovered at the end of the experiment and used again in another reaction or analytical procedure.

A considerable amount of information is contained in the time-dependent static light scattering (TDSLS) signature corresponding to the reaction, and such signatures are explored for a variety of acrylamide polymerization reactions in this work. A precedent for this approach was the work of Chu and Lee,[8] who made single sample in situ light scattering measurements, but did not seek an interpretation of the time-dependent scattering behavior in terms of the properties of the polymerization reaction.

A more conventional approach to screening is to perform sequential gel permeation chromatography (GPC) measurements on each endproduct of multiple reactions. While useful, this approach takes considerable postreaction time, even if higher speed and lower resolution GPC is employed (i.e., using shorter columns), and provides only information on the endproducts and not on kinetics or mechanisms, and is usually costly to implement and maintain. To obtain kinetic information, other elaborate chromatographic systems can be used, such as gas chromatography connected to a parallel synthesis workstation equipped with an autosampler. Numerous spectroscopic readers are also available, but samples must normally be processed prior to any analysis.

Other in situ methods for monitoring polymerization reactions exist, but have not been brought to the level of performing multiple simultaneous measurements. One of the most successful in situ methods is infrared spectroscopy, with near-, mid-, and far-IR each having a particular advantage.[9−14] Other in situ methods include densitometry[15] and rheom-

---

* Corresponding author.
† Current address: Combinatorial Catalysis Team, UMR6509 Université de Rennes, 35042 Rennes, France.

etry.[16,17] All of these methods require an empirical or chemometric model for the interpretation of the data stream.

Light scattering has long been recognized as a model-independent, absolute means of characterizing polymer mass, spatial dimensions, and interactions (these latter measured by the second, third, and higher virial coefficients, A_2, A_3, etc.) in dilute solutions. Because polymerization reactions generally use high concentrations of monomer, which produce correspondingly high concentrations of polymer, A_2 and A_3 effects quickly come to dominate the scattering behavior. Using automatic, continuous extraction and high dilution, automatic continuous online monitoring of polymerization reactions (ACOMP)[18,19] has been recently developed as an absolute, model-independent method to follow M_w, monomer and comonomer conversion, intrinsic viscosity, measures of polydispersity, and other characteristics. It is not practical, economical, or necessary to apply ACOMP to many simultaneous reactions when the goal is qualitative and semiquantitative high-speed screening.

The object of this work is to give examples of SMSLS data and their interpretation for a variety of polymerization conditions for a chosen reaction, the chemically initiated polymerization of acrylamide in aqueous solution. The endproducts of each reaction were also measured by gel permeation chromatography to cross-check the SMSLS results. This work should set the stage for approaching a wide variety of possible reactions using SMSLS.

Time-Dependent Static Light Scattering (TDSLS) Signatures from Polymerizing Solutions. Recently, the groundwork for combining virial coefficient and dilute/semidilute crossover expressions for light scattering with different types of polymerization kinetics was published.[20] This analysis included free radical polymerization for the cases of both constant and decreasing weight average molecular mass M_w, during the reaction, as well as dead-end reactions.[21] Additionally, predictions were made concerning controlled radical polymerization (CRP),[22−24] when it resembles a living type reaction. Comparing experimental data to the various models, including crossover expressions,[25] it was determined that Zimm's virial coefficient expansion for light scattering[26] in the limit of $q = 0$ (q is the amplitude of the scattering vector) was the most robust:

$$\frac{Kc}{I_R} = \frac{1}{M_w} + 2A_2c + 3A_3c^2 + \dots \tag{1}$$

where I_R is the absolute Rayleigh scattering ratio (cm^{-1}) measured by the SMSLS instrument, c is the concentration of polymer (g/cm^3), A_2 and A_3 are the second and third virial coefficients, respectively, and K is an optical constant, given for vertically polarized incident light by

$$K = \frac{4\pi^2 n^2 (\partial n/\partial c)^2}{N_A \lambda^4} \tag{2}$$

I_R is computed from the SMSLS scattering voltages by taking the ratios of these to that scattered by toluene, and multiplying by $I_{R,toluene} = 1.069 \times 10^{-5}$ cm^{-1} for 677 nm incident light on toluene at 25 °C.

The values of A_2 for the polyacrylamide (PAA) are related to the mass according to the experimentally determined expressions found earlier,[20]

$$A_2 = 0.00425 M_w^{-0.167} \tag{3}$$

and A_3 is related to A_2 via the theoretical (monodisperse) expression

$$A_3 = \epsilon \frac{5MA_2^2}{8} \tag{4}$$

where $\epsilon = 0.095 +/ 0.03$ was found in the same work, by substituting the experimentally found M_w in place of M in eq 4.

In ref 20, the only kinetic model for molar monomer conversion $f(t)$ considered was the first-order case, where

$$f(t) = 1 - \exp^{-\alpha t} \tag{5}$$

where $\alpha = k_p[R]$, and k_p is the propagation rate constant and $[R]$ is the molar concentration of the polymeric radical. When this expression applies, and M_w is approximated as constant throughout the reaction, the fit to the SMSLS data involves only two adjustable parameters, M_w and α, because A_2 and A_3 are expressed in terms of M_w, by eqs 3 and 4. For deviations from either constant M_w or first-order conversion, additional parameters can be added to the fitting procedure, although this necessarily increases the error bars on each parameter thus found.

In this work, two sets of experimental TDSLS signatures from polymerization reactions, carried out eight at a time, are shown and are compared to a "library" of theoretical free radical TDSLS polymerization signatures shown in Figure 1a,b. These signatures are computed from the time-dependent form of eq 1

$$I_R(t) = \frac{K(t)\,c(t)}{\dfrac{1}{M_w(t)} + 2A_2(t)\,c(t) + 3A_3(t)\,c(t)^2 + \dots} \tag{6}$$

where $K(t)$ does not normally change measurably during conversion, and $c(t) = c_{m,0}\,f(t)$, where $c_{m,0}$ is the initial monomer concentration.

Four cases are shown in Figure 1a,b, where the curves in the figure are the same, but the time scale in Figure 1b is 10 times shorter than that in Figure 1a, to show how the different signatures distinguish themselves from each other on both short and long time scales. Included are the cases of free radical polymerization and first-order monomer conversion with $M_w = $ constant (10^6 g/mol) at low (3.5 $\times$ 10^{-3} g/cm^3) and high concentration (3.5 $\times$ 10^{-2} g/cm^3), curves I and II, respectively, and with high concentration but impurity present that competes for radicalized, decomposed initiator, shown in curve III. Curve IV shows the case of high concentration, but where M_w starts high (7 $\times$ 10^6) and drops to 10^6 during the reaction. All curves, except the one at low concentration, show maxima in I_R, but with distinctly different details. Curve IV, for example, shows a "valley" after the initial maximum on the long time scale, whereas curve III shows
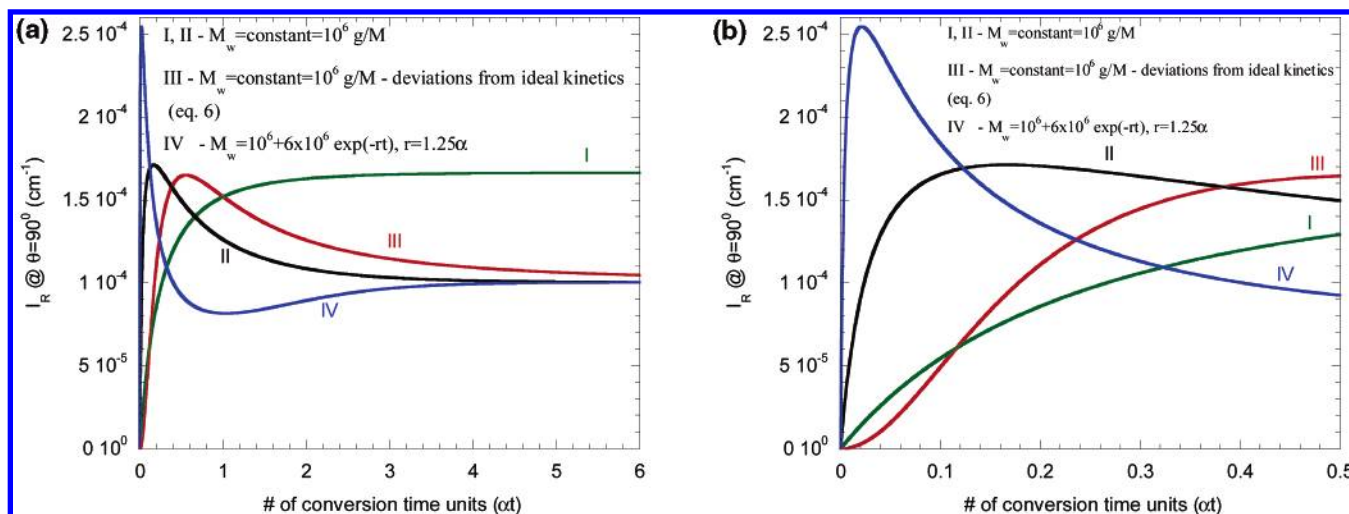
Figure 1. (a) "Library" of theoretical time-dependent static light scattering (TDSLS) signatures for a variety of free radical polymerization conditions, described in the text. (b) TDSLS signatures from (a) on 1/10 the time scale to illustrate additional features of each signature.

a concave upward initial curvature on the short time scale for the case where impurity is present.

It is noted that the time-dependence of M_w varies widely for different free radical reactions and can increase, decrease, or remain constant, depending on several factors.

Detailed conversion curves for the impurity effect were found in ref 19 and elsewhere. A good approximation to this effect is given by

$$f(t) = \frac{at}{1 + at}(1 - \exp^{-\alpha t}) \qquad (7)$$

where a is a constant. Equation 7 was used in conjunction with eqs 3, 4, and 6 to generate signature III in Figure 1a,b.

The variety of signatures in Figure 1a,b stems from the interplay between the starting monomer concentration, conversion kinetics, any change in M_w during polymerization (e.g., increasing with conversion for CRP, and decreasing with conversion for free radical polymerization in the case of a long-lived initiator), as well as deviations in kinetics, such as that given by eq 7.

Experimental Section

The SMSLS System. The SMSLS prototype used in this work can accommodate eight independent samples. In principle, there is no limit to the number of samples that can be incorporated into an SMSLS device, although a practical limitation per linear CCD array is around 50. The device uses inexpensive 1 cm square borosilicate sample cuvettes as minireactors, which can be inserted into the device, and later be either cleaned or discarded. A 25-mW, 677-nm vertically polarized diode laser (LaserMax, Rochester, NY) was used as the light source and was split with a 50% splitter into two beams. Each beam was incident on identical sample holders machined from black Nylon, containing milled recesses for each of four cells, and fluid communication channels among the cells, so that an index matching fluid (toluene in this case) bathes the exterior of the cells. This SMSLS device is hence a hybrid of serial and parallel operation, there being two parallel sample banks, each with four sample cells in series. Optical fibers (Polymi-

cro Technology) of diameter 0.48 mm collected the scattered light at a scattering angle of 90° from each cell and were led to a Hammamatsu charge coupled device (BC-CCD, HC230-0907). Scattered intensity data from the CCD were continuously monitored via a Labview data interface. Data reduction software was written separately by the authors.

The current SMSLS device also has flow cells of ~0.5 mL each. These were not used in the current experiments, but could prove useful in other situations as discussed in the Outlook section below. Scheme 1 shows the prototype system used, in which can be seen the eight reaction cells; fiber optic pick-up for each cell, which all run into a harness to the CCD detector; and the laser beam splitter. Not shown in the scheme is the nitrogen-purging apparatus and sealed septum for each cell. The overall modularity of the SMSLS design should also lend itself to robotic automation, if desired.

A detailed study of reflection/scattering losses from cell to cell for cells in series was given in ref 7. For borosilicate glass ($n_g = 1.533$) and toluene as index matching fluid ($n_t = 1.496$), the reflection loss after passing through three cells (i.e., entering the fourth) is a negligible 1.5%, and the loss due to scattering is even smaller. If we assume a typical scattering value in the polymer solution on the order of the Rayleigh ratio of toluene, then after passing through three cells the scattering loss is only 0.025%. A proviso is that, if any turbidity develops, the cells down-beam from the first turbid cell will no longer give valid data. In such systems, a purely parallel mode for the SMSLS cells is needed and is easily configured.

Acrylamide Polymerization Experiments. Ultrapure electrophoresis grade acrylamide (Aam) and potassium persulfate (KPS, 99% minimum purity) were from Polysciences, Inc., and N,N,N′,N′-tetramethylethylenediamine (TMEDA, 99% minimum purity) was from Spectrum Quality Products, Inc. All reagents were used without further purification. Solutions of each reagent were made in ultrapure deionized water and purged under nitrogen constantly, using a device to distribute the gas flow to each SMSLS sample cell. Aam concentrations were from 0.0039 to 0.0350 g/mL,

Scheme 1. The SMSLS Prototype Used for This Work
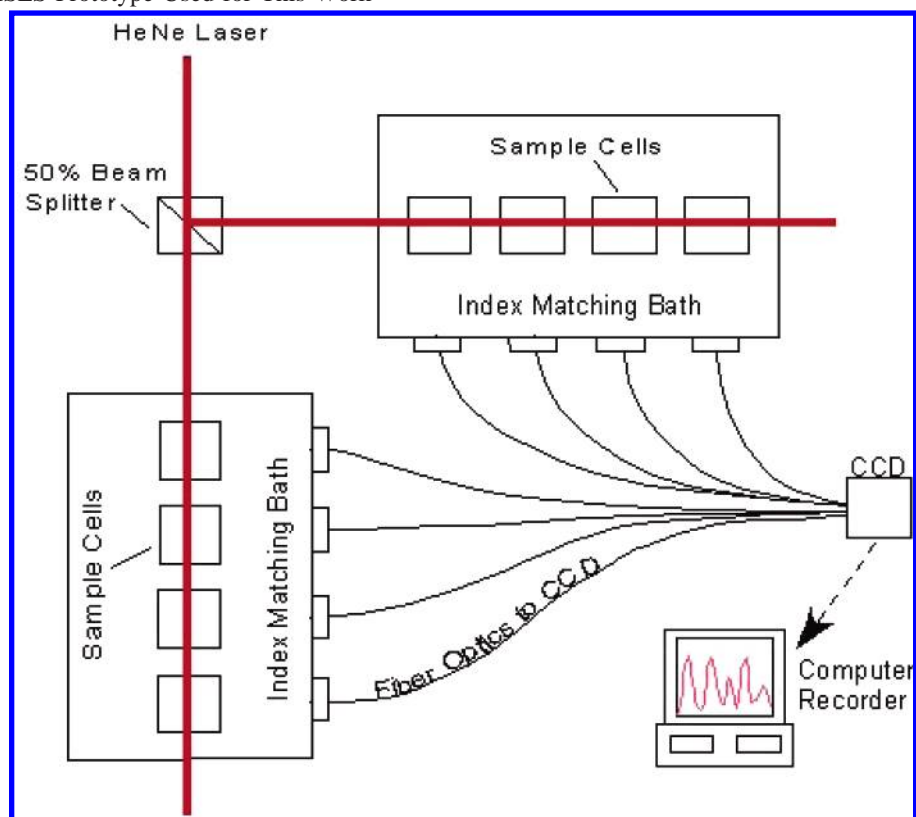
and concentrations used for KPS and TMEDA were from 0.00037 to 0.0033 mol/L. The solutions were filtered through a 0.22-μm Millipore filter. Next, 3 mL of monomer solution was injected into each removable borosilicate SMSLS cuvette, functioning as reactors, then 0.1 mL of KPS was injected, and finally, 0.1 mL of TMEDA solution was injected. The ratio of the catalytic initiator system KPS/TMEDA in each reactor was 1:1 in mol. The polymerization reactions were carried out, eight at a time in the SMSLS device, at ambient temperature, $T = \sim 25$ °C, under constant nitrogen purge and constant stirring.

The scattering volume in each SMSLS cell was on the order of 10 nL and, together with recognition of any spurious scattering peaks in the data, allowed for virtually complete elimination of scattering due to "dust" and other impurities. While more scattering angles would be preferable for extrapolations to $q = 0$, the current design geometry did not allow this. Hence, while this work is focused on the extraction of reaction rate constants and average polymer masses during polymerization, the current apparatus does not permit structural determinations of the polymer to be made.

The multidetector GPC system used to analyze reaction endproducts consisted of an Agilent 1100 isocratic pump, a Shodex HB-806 column, a Brookhaven Instruments BI-MwA multiangle light scattering detector, a home-built single capillary viscometer,[27] and a Shimadzu RID-10A refractometer. The eluent was aqueous 0.1 M NaCl, and a flow rate of 0.8 mL/min was used.

Results

Figure 2a shows raw scattering data, expressed as I_R (cm^{-1}) for eight simultaneous Aam reactions, whose conditions are given by the code in Table 1. Figure 2b shows a second experiment with another set of eight reactions, using the same code as in Table 1.

In each case in Figure 2a,b, the experimental TDSLS signature corresponds well to one of the "library" signatures in Figure 1a,b. Table 2 shows the signature type of each reaction according to Figure 1a,b, and the resulting M_w and rate constant α for each fit. The fits themselves are shown together with the data in Figure 2a,b. Also shown in Table 2 are the results from multi-detector GPC, carried out on the final products of each reaction. Table 3 gives the corresponding results for the experimental signatures from Figure 2b.

It is notable that both reactions CAA1 and CAA2 in Figure 2a show the characteristic initial upturn in I_R that occurs when initial impurities compete with monomers for free radicals resulting from the initiator decomposition. This is most likely to occur when there are impurities present, such as incompletely purged O$_2$, and when the monomer concentration is low. Signature CBB2 in Figure 2b also shows this effect, and CBB1 gives an even more pronounced effect of this type.

Reactions AAA1 and AAA2 in Figure 2a, and reactions AAA, ABB1, and ABB2 in Figure 2b, which have the largest initial amount of monomer, show the characteristic maxima of I_R predicted by the signatures in Figure 1a,b, whereas in the cases of lower concentration a plateau is reached. The fact that virtually all of the signatures are well fit with a single M_w suggests that M_w is largely constant throughout the reactions. Figure 1a,b shows that a decreasing M_w should lead to a "valley" in I_R after the maximum is reached. A case of this is seen in reaction ABB2 in Figure 2b.

Referring to Tables 2 and 3, it is seen that the SMSLS results, given by $M_{w,fit}$, are in fair agreement with the GPC
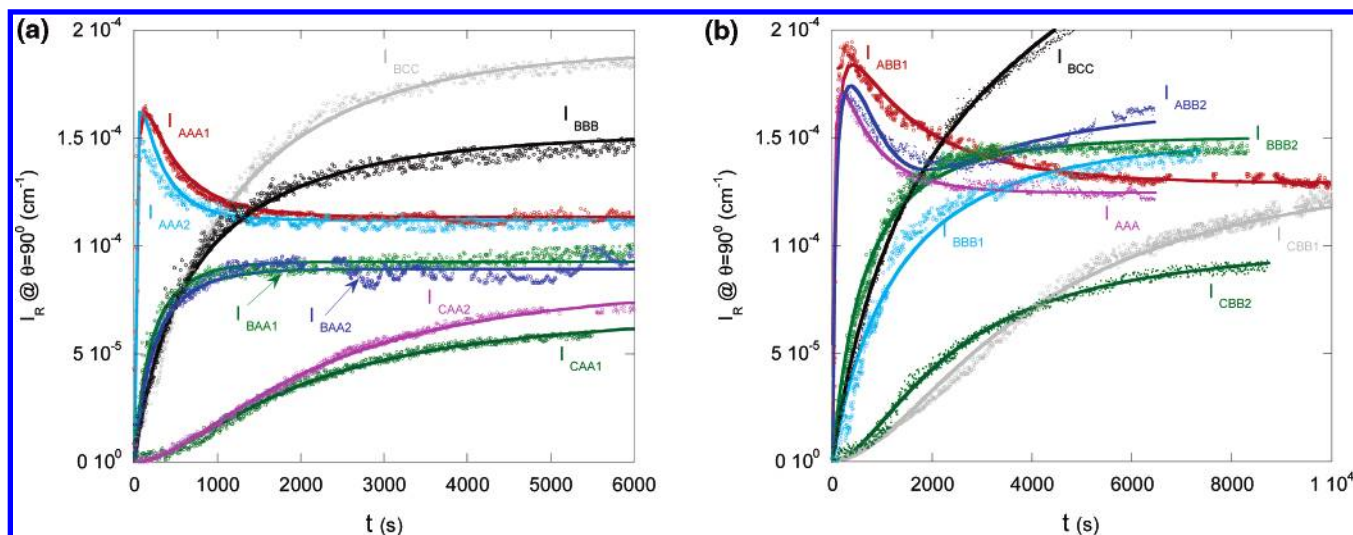
Figure 2. (a) Experimental TDSLS signatures (expressed as absolute Rayleigh ratio, I_R) for eight simultaneous acrylamide polymerization experiments. The fits according to the parameters in Table 2 are also shown. (b) TDSLS signatures for an additional eight simultaneous acrylamide polymerization experiments. The fits according to the parameters in Table 3 are also shown.

Table 1. Summary of Reactions in Figure 2a,b

	monomer (g/mL/M)	initiator (g/mL/M)	catalyst (g/mL/M)
AAA	0.0355/0.5	$9.03 \times 10^{-4}/0.33 \times 10^{-2}$	$3.87 \times 10^{-4}/0.33 \times 10^{-2}$
ABB	0.0355/0.5	$2.26 \times 10^{-4}/8.33 \times 10^{-4}$	$9.68 \times 10^{-5}/8.33 \times 10^{-4}$
BAA	0.0088/0.125	$9.03 \times 10^{-4}/0.\ 33 \times 10^{-2}$	$3.87 \times 10^{-4}/0.\ 33 \times 10^{-2}$
BBB	0.0088/0.125	$2.26 \times 10^{-4}/8.33 \times 10^{-4}$	$9.68 \times 10^{-5}/8.33 \times 10^{-4}$
BCC	0.0088/0.125	$1.00 \times 10^{-4}/3.70 \times 10^{-4}$	$4.30 \times 10^{-5}/3.70 \times 10^{-4}$
CAA	0.0039/0.55	$9.03 \times 10^{-4}/0.33 \times 10^{-2}$	$3.87 \times 10^{-4}/0.33 \times 10^{-2}$
CBB	0.0039/0.055	$2.26 \times 10^{-4}/8.33 \times 10^{--4}$	$9.68 \times 10^{-5}/8.33 \times 10^{-4}$

Table 2. M_w and α as Obtained from Fits to $I_R(t)$ for the Data from Figure 2a (M_w and α Were the Only Fitting Parameters)[a]

experiment label from Table 1	M_w (GPC)	M_w (GPC − 90°)	M_w (fit)	α (s^{-1}))	signature type from Figure 1a,b
AAA1	1.05×10^6	5.63×10^5	6.923×10^5	1.817×10^{-3}	II
AAA2	9.84×10^5	6.70×10^5	7.325×10^5	2.757×10^{-3}	II
BCC	7.76×10^5	5.54×10^5	1.527×10^6	6.753×10^{-5}	I
BBB	4.83×10^5	3.90×10^5	4.800×10^5	2.663×10^{-4}	I
BAA1	3.33×10^5	2.42×10^5	1.173×10^5	2.277×10^{-3}	I
BAA2	2.76×10^5	2.25×10^5	1.092×10^5	2.052×10^{-3}	I
CAA1	1.38×10^5	1.33×10^5	1.652×10^5	6.945×10^{-4}	III
CAA2	1.73×10^5	1.47×10^5	2.232×10^5	5.127×10^{-4}	III

[a] Also shown are GPC values of M_w on the end products of each reaction, both from extrapolation of multi-angle light scattering to $q = 0$, M_w (GPC) and at a fixed scattering angle of 90°, M_w (GPC − 90°). The signature types, according to Figure 1a,b, are also shown.

Table 3. M_w and α as Obtained from $I(t)$ for the Data from Figure 2b[a]

experiment label from Table 1	M_w (GPC)	M_w (GPC − 90°)	M_w (fit)	α (s^{-1})	signature type from Figure 1a,b
ABB1[b]	2.270×10^6	9.93×10^5	1.024×10^6	5.255×10^{-4}	II
ABB2	2.110×10^6	1.055×10^6	9.933×10^5	4.970×10^{-4}	IV
AAA[b]	1.750×10^6	8.745×10^5	7.627×10^6	1.165×10^{-3}	II
BCC[b]	8.470×10^5	5.932×10^5	1.450×10^6	5.638×10^{-5}	I
BBB1[c]	5.354×10^5	3.960×10^5	4.690×10^5	1.463×10^{-4}	I
BBB2	4.860×10^5	3.928×10^5	4.610×10^5	2.895×10^{-4}	I
CBB1	2.330×10^5	1.920×10^5	2.230×10^5	1.957×10^{-4}	III
CBB2	1.140×10^5	1.015×10^5	2.657×10^5	1.992×10^{-4}	III

[a] Except where noted, M_w and α were the only fitting parameters. [b] ϵ was used as a third adjustable parameter. [c] [Aam] = 0.1 M, [initiator] = 6.6×10^{-3} M, [catalyst] = 6.6×10^{-3} M.

values of M_w in most cases. These fits were made to the I_R in Figure 2a with only M_w and α as the free parameters, with ϵ held fixed at the experimental value of 0.095. A few exceptions to this are noted by footnote a in Table 3, for which ϵ was also used as a fitting parameter, and generally yielded ϵ within error bars of the experimental value. In Figure 2b, eq 7 was used for ABB2, introducing the additional parameter a. Tables 2 and 3 show both M_w from GPC with the usual extrapolation of the multi-angle scattering data to $q = 0$, labeled M_w (GPC), as well as the GPC value

for the apparent M_w obtained by using only the 90° scattering value, labeled M_w (GPC, 90°). Because the SMSLS reports only the 90° value, these latter two are most properly compared. As M_w increases, the angular extrapolation becomes more important, and the SMSLS fit for M_w will increasingly underestimate the $q = 0$ value of M_w. Corrections involving the mean square radius of gyration $\langle S^2 \rangle$ were introduced in ref 20, but are not pursued here. For screening purposes, the SMSLS gives a reasonable estimate of M_w, rather than a highly accurate value. Extensive error analysis was presented in ref 20 and is not detailed here.

The rate constants α given in Table 2 vary as would be expected and span the range of 6×10^{-5} to 2.8×10^{-3} s^{-1}. The higher is the initiator concentration, the faster is the rate, although reactions with high initiator (A) and low monomer (C) are intermediate in value, possibly because a smaller fraction of monomer is radicalized during initiator decay on account of its lower concentration. It is noted that while GPC provides a useful cross-check on SMSLS, it is silent on kinetics, unless one were to laboriously make manual aliquot extractions during the reaction and make a GPC analysis for each.

Outlook for SMSLS for Use with Other Types of Polymerization Reactions. The reactions in this work were carried out with a relatively low concentration of monomer, a maximum of 3.5% by mass, which nonetheless brought many of the reactions into the semidilute regime. In reactions involving higher monomer concentration, or even in bulk, the semidilute regime will be quickly reached. It will then be difficult to extract much information on the majority part of the reactions. In terms of screening, however, the detailed information on rate and M_w furnished in the early reaction stages will still be useful, because it will show if the reaction is occurring at all, what the initial rate and M_w are, and whether there are any mechanistic peculiarities, which are often expected to appear early in the reaction, for example, impurity effects, as seen in reactions CAA1 and CAA2 in Figure 2a, and in CBB1 and CBB2 in Figure 2b.

A means of extending the reach of SMSLS into later reaction stages for concentrated and bulk reactions, as well as to reactions requiring more complicated minireactors than might be accommodated by sample cuvettes alone, might combine the ACOMP concept of automatic extraction and dilution[18,19,28] to many parallel minireactors, and use, for example, a multi-head peristaltic pump and "y"-dividers (or solenoid driven fluidic valves) to feed the multiple flow cells on the SMSLS. This would consume liquid from each reactor, but typically only on the order of ∼10 μL/min.

Although these reactions were performed at room temperature, it is technically straightforward to equip each cell with its own Peltier heater/cooler, or to control whole blocks of SMSLS cells with these or other types of heating elements. In the case where the flow cells are used in the ACOMP scheme, the minireactors would be temperature controlled, and then there would be no need for temperature control of the SMSLS device, as this would just continuously measure the continuously diluted, quenched stream from the reactors.

A caveat for the applicability of SMSLS is that solutions must remain optically clear during at least the initial phases of the reaction. Hence, cloudy or colored media, or heterogeneous phase reactions, are not readily amenable to SMSLS in its current form. Schemes involving manipulations of prepared microstreams, such as phase inversion with surfactants, dissolution of slurries, filtration, and separation of organic/aqueous phases, may extend the reach of flow-cell-based SMSLS in some of the more adverse polymerization conditions.

Using standard laboratory procedures, SMSLS is a safe technique. Given the high-throughput capability, it is also inexpensive on a cost per sample basis.

Besides measuring rate and M_w, the SMSLS monitoring would also be sensitive to processes such as microgelation during polymerization, because light scattering is sensitive to even small amounts of aggregation. By the same token, SMSLS can be used to conveniently monitor the stability over time of the endproducts, as it is well known that polymers in solution are often only quasi-stable and subject to aggregation and phase separation.

Conclusions

Time-dependent static light scattering signatures of solutions undergoing polymerization reactions, obtained using SMSLS, are shown to contain an abundance of qualitative and semiquantitative information on both the kinetics of the reactions and the approximate M_w of the polymers produced. While SMSLS does not attempt to compete with absolute monitoring techniques, such as ACOMP, nor provide detailed polymer mass distributions such as from GPC, it nonetheless should prove useful for screening many reactions simultaneously, whence the most promising reactions screened could be subjected to more rigorous further testing and characterization. It has been shown that very robust fits are obtained with only two adjustable parameters, M_w and reaction rate α, which should prove to be among the most valuable characteristics for screening purposes.

SMSLS should have wide applicability for screening polymerization reactions, as well as parallel testing of the long-term stability of polymer solutions against such phenomena as aggregation, phase separation, and degradation.

References and Notes

(1) Adams, N.; Schubert, U. S. *J. Comb. Chem.* **2004**, *6*, 12.
(2) Reynolds, C. H. *J. Comb. Chem.* **1999**, *1*, 297.
(3) Hodges, J. C.; Harikrishnan, L. S.; Ault-Justus, S. *J. Comb. Chem.* **2000**, *2*, 80.
(4) Tuchbreiter, A.; Marquardt, J.; Zimmermann, J.; Walter, P.; Mulhaupt, R.; Kappler, B.; Faller, D.; Roths, T.; Honerkamp, J. *J. Comb. Chem.* **2001**, *3*, 598.
(5) Reed, W. F. U.S. patent no. 6,618,144, 2003.
(6) Drenski, M. F.; Reed, W. F. *Polym. Mater. Sci. Eng.* **2003**, *88*, 304.
(7) Drenski, M. F.; Reed, W. F. *J. Appl. Polym. Sci.* **2004**, *92*, 2724.
(8) Chu, B.; Lee, D. C. *Macromolecules* **1984**, *17*, 926.
(9) Cherfi, A.; Févotte, G. *Macromol. Chem. Phys.* **2002**, *203*, 1188.
(10) Pasquale, A. J.; Long, T. E. *Macromolecules* **1999**, *32*, 7954.

(11) Long, T. E.; Liu, H. Y.; Schell, B. A.; Teegarden, D. M.; Uerz, D. S. *Macromolecules* **1993**, *26*, 6237.

(12) Shaikh, S.; Puskas, J. E. *Polym. News* **2003**, *28*, 71.

(13) Storey, R. F.; Donnalley, A. B.; Maggio, T. L. *Macromolecules* **1998**, *31*, 1523.

(14) Olinga, A.; Winzen, R.; Rehage, H.; Siesler, H. W. *J. Near Infrared Spectrosc.* **2001**, *9*, 19.

(15) Ballard, D. G. H.; van Lienden, P. W. *Makromol. Chem.* **1972**, *154*, 177.

(16) Brand, O.; English, J. M.; Bidstrup, S. A.; Allen, M. G. *Sens. Actuators* **1997**, *1*, 121.

(17) Ponnuswamy, S.; Shah, S. L.; Kiparissides, C. *J. Appl. Polym. Sci.* **1986**, *32*, 3239.

(18) Florenzano, F. H.; Strelitzki, R.; Reed, W. F. *Macromolecules* **1998**, *31*, 7226.

(19) Giz, A.; Giz, H.; Brousseau, J. L.; Alb, A. M.; Reed, W. F. *Macromolecules* **2001**, *34*, 1180.

(20) Alb, A. M.; Mignard, E.; Drenski, M. F.; Reed, W. F. *Macromolecules* **2004**, *37*, 2578.

(21) Tobolsky, A. V.; Gobran, R. H.; Boehme, R.; Schaffhauser, R. *J. Am. Chem. Soc.* **1963**, *85*, 2336.

(22) Matyjaszewski, K., Davis, T. M., Eds. *Handbook of Radical Polymerization*; John Wiley & Sons: Hoboken, 2002.

(23) Hawker, C. J.; Bosman, A. W.; Harth, E. *Chem. Rev.* **2001**, *101*, 3661.

(24) Davis, T. P.; Haddleton, D. M.; Richards, S. N. *J. Macromol. Sci., Rev. Macromol. Chem. Phys.* **1994**, *C34* (2), 243.

(25) Berry, G. C. *Adv. Polym. Sci.* 1**994**, *114*, 233.

(26) Zimm, B. H. *J. Chem. Phys.* **1948**, *16*, 1093.

(27) Norwood, D. P.; Reed, W. F. *Int. J. Polym. Anal. Charact.* **1997**, *4*, 99.

(28) Reed, W. F. U.S. patent no. 6,653,150, 2003.